# ELECTRONIC SUPPLEMENTARY INFORMATION

# Highly differentiated multi stimuli-responsive fluorescence performance of tetraphenylethylene-containing styrene-maleic acid copolymers induced by macromolecular architecture control

*Ranran Gao[a], Xiaoning Guo[a], Li Wang\*[a], Wantai Yang\*[abc]*

[a] *State Key Laboratory of Chemical Resource Engineering, Beijing University of Chemical Technology, Beijing 100029, China*

[b] *Beijing Engineering Research Center for the Syntheses and Applications of Waterborne Polymers, College of Materials Science and Engineering, Beijing University of Chemical Technology, Beijing 100029, China*

[c] *Beijing Advanced Innovation Centre for Soft Matter Science and Engineering, Beijing 100029, China*
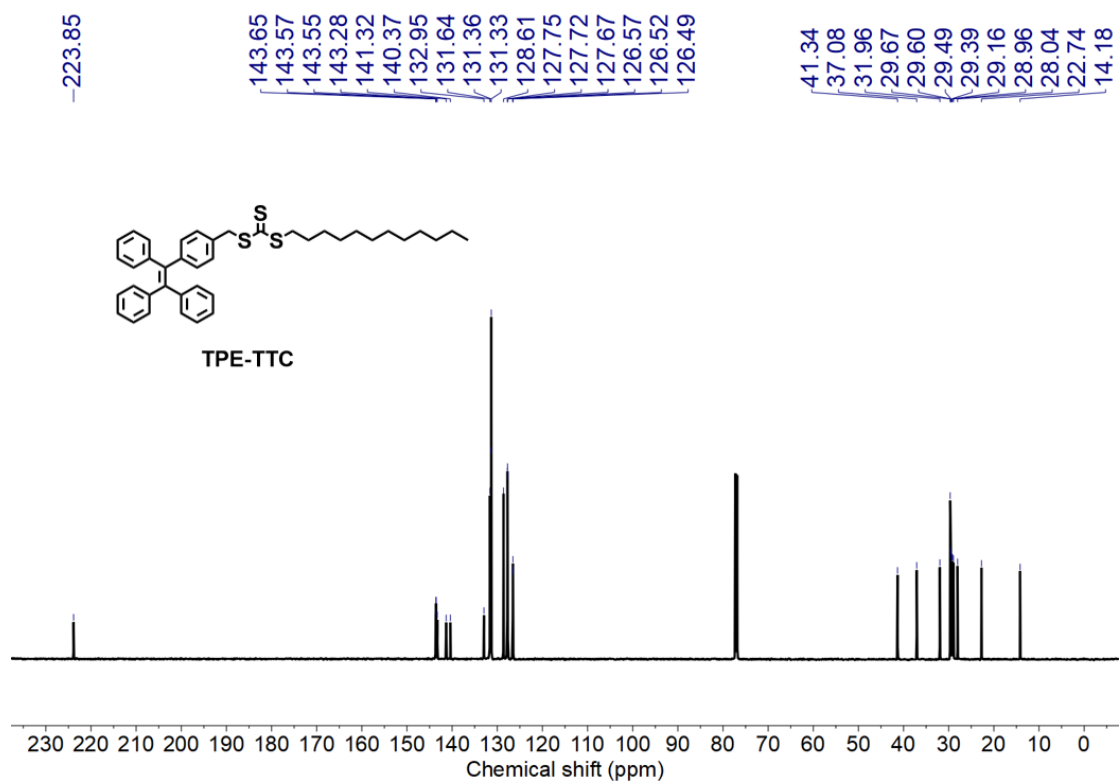
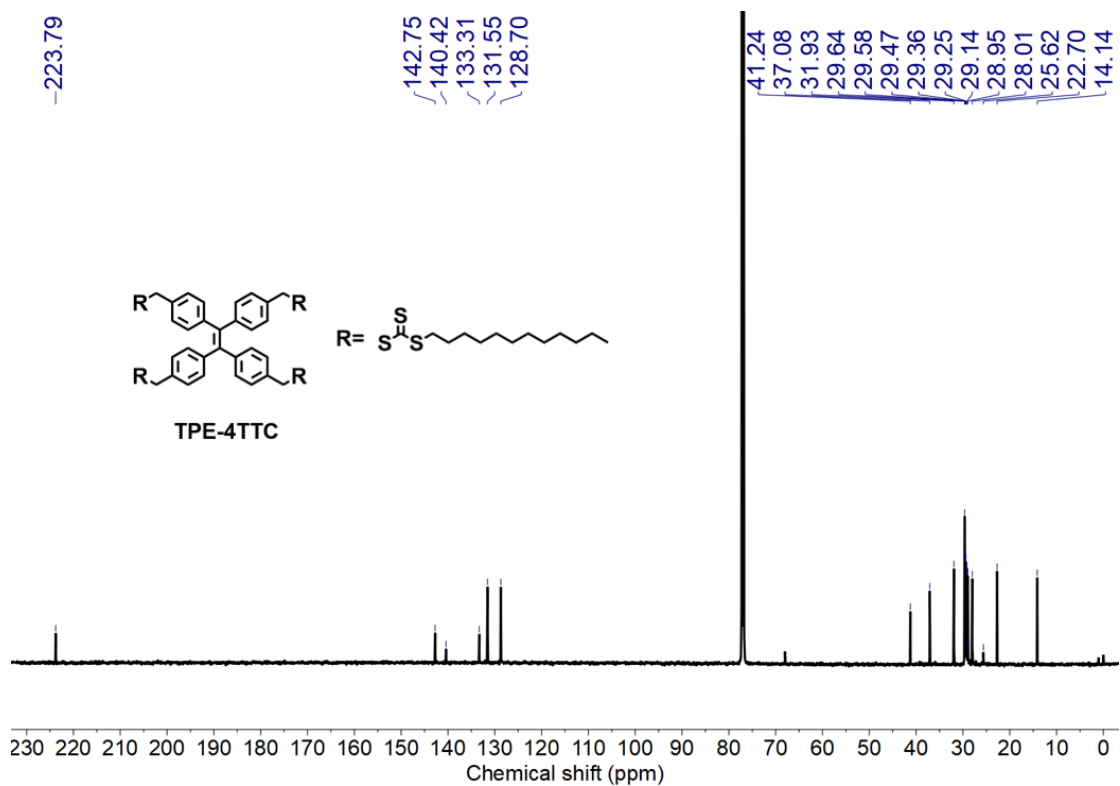**Figure. S1** $^{13}$C NMR spectra of TPE-TTC in CDCl$_3$.



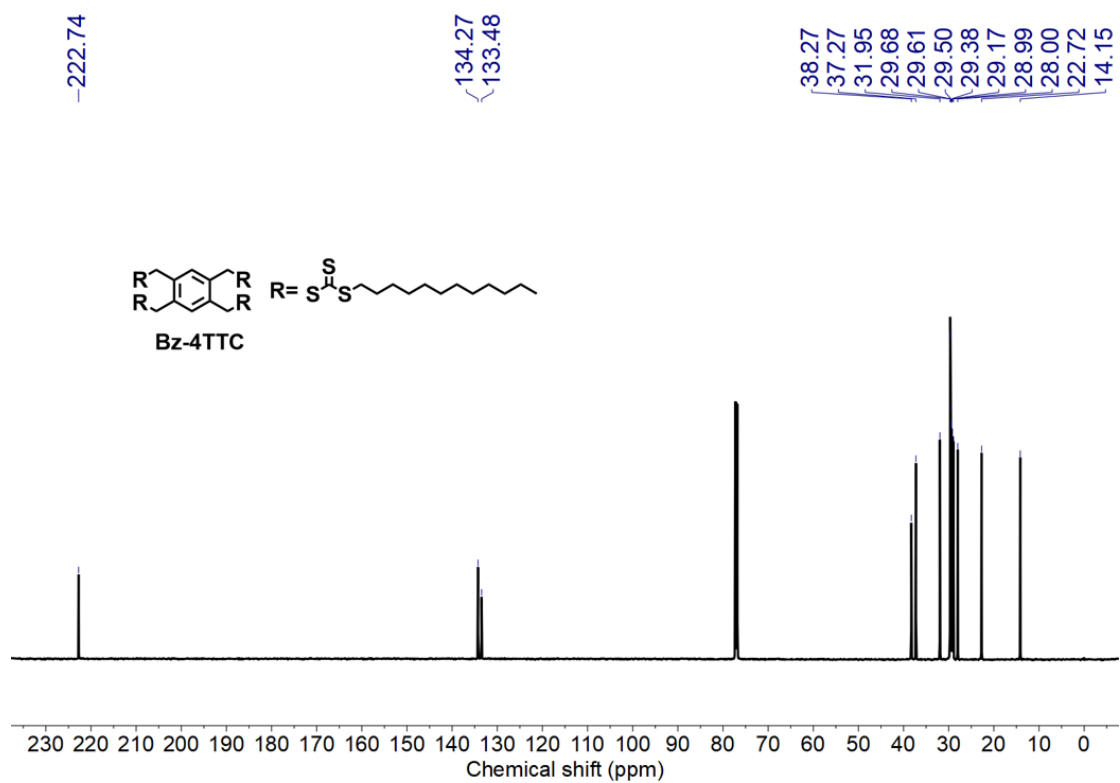**Figure. S2** $^{13}$C NMR spectra of TPE-4TTC in CDCl$_3$.

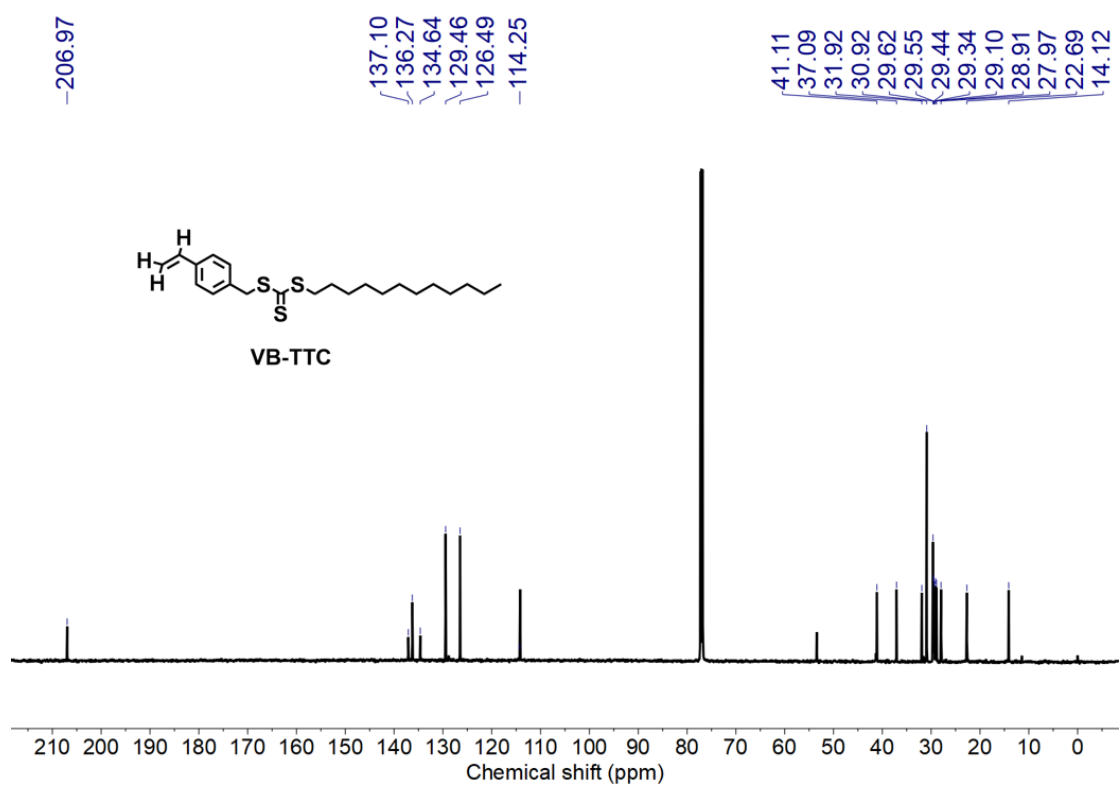**Figure. S3** $^{13}$C NMR spectra of Bz-4TTC in CDCl$_3$.



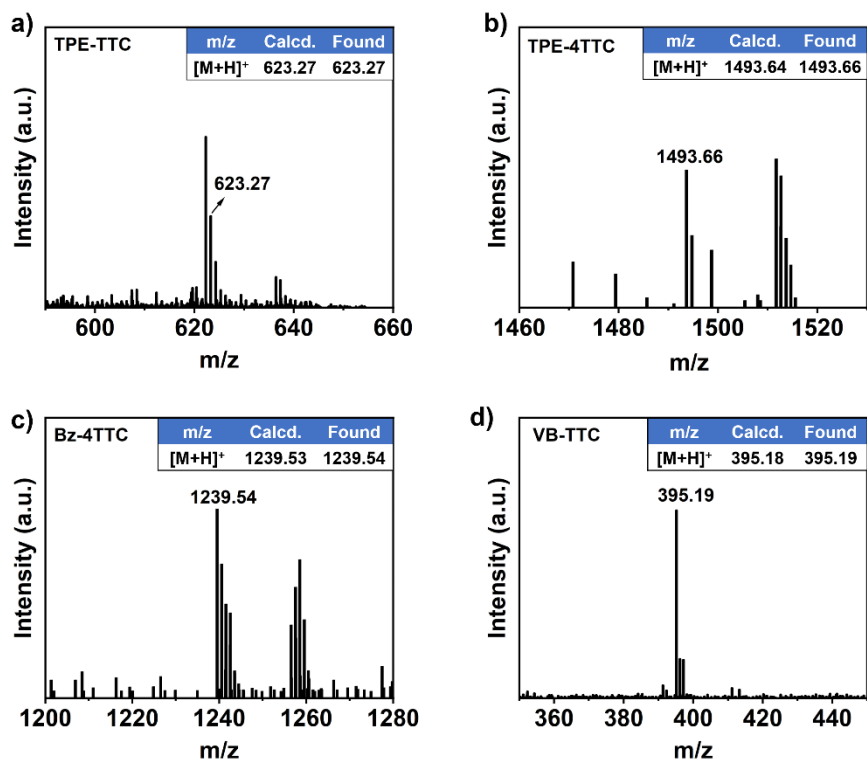**Figure. S4** $^{13}$C NMR spectra of VB-TTC in CDCl$_3$.

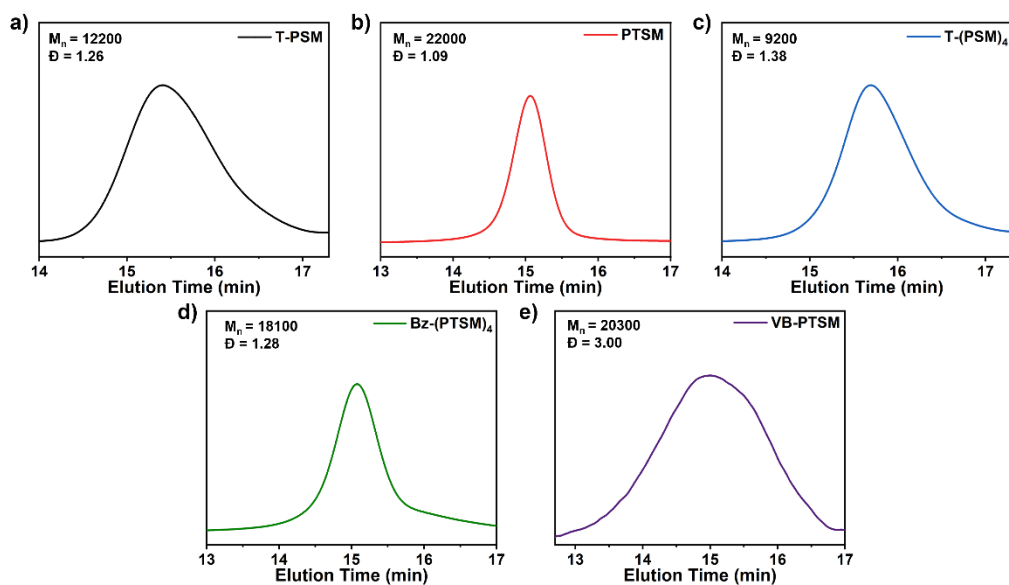**Figure. S5** ESI MS spectra of (a) TPE-TTC, (b) TPE-4TTC, (c) Bz-4TTC, (d) VB-TTC.



**Figure. S6** GPC traces of (a) T-PSM, (b) PTSM, (c) T-$(PSM)_4$, (d) Bz-$(PSM)_4$ and (e) VB-PTSM.
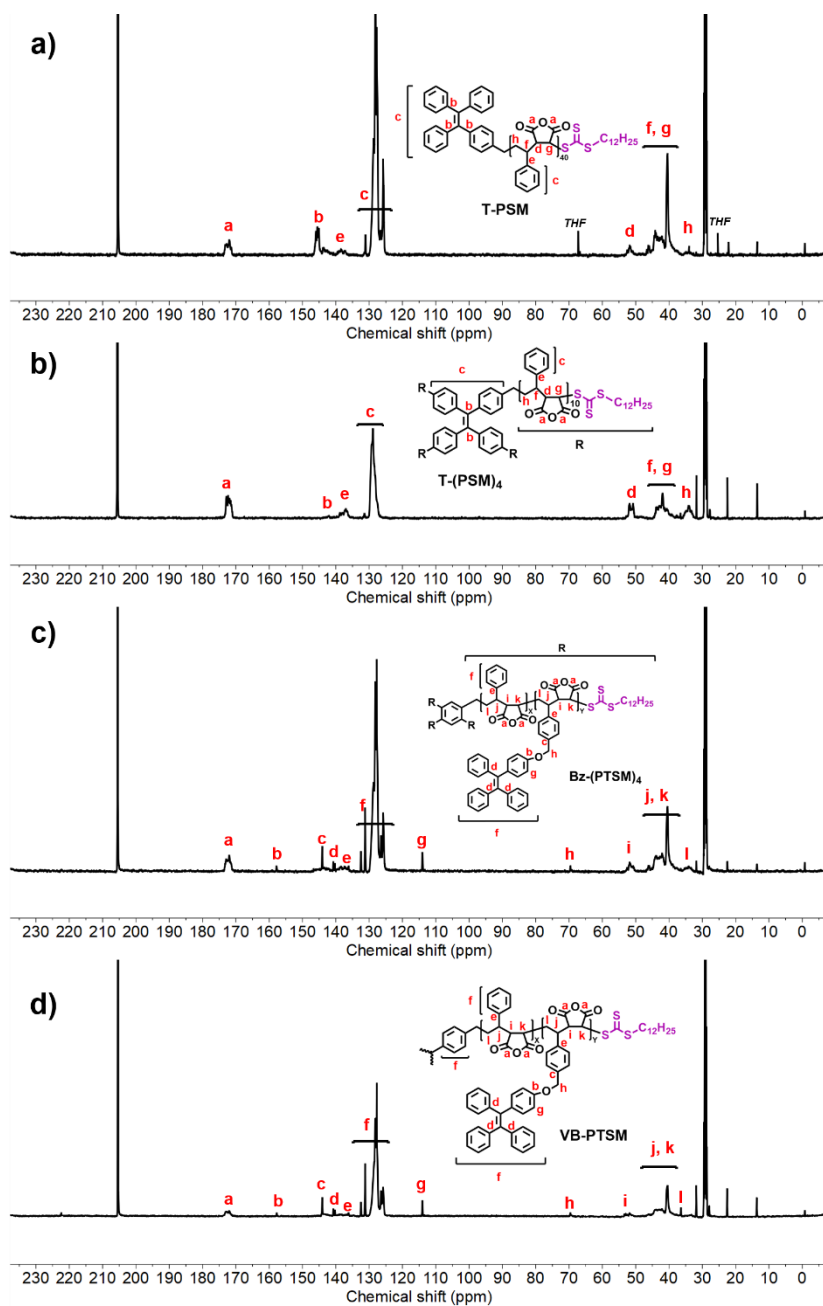
**Figure. S7** ^{13}C NMR spectra of (a) T-PSM, (b) T-(PSM)$_4$, (c) Bz-(PTSM)$_4$, and (d) VB-PTSM in CD$_3$COCD$_3$. The quaternary carbon (Ce) of styrene units resonates at 141.5-147.5 ppm in non-alternating and semi-alternating triads, which is not present in the above spectrum. The peak of Ce attributed to the alternating triad of MAH-St-MAH[1] at 137 ppm can be clearly seen.
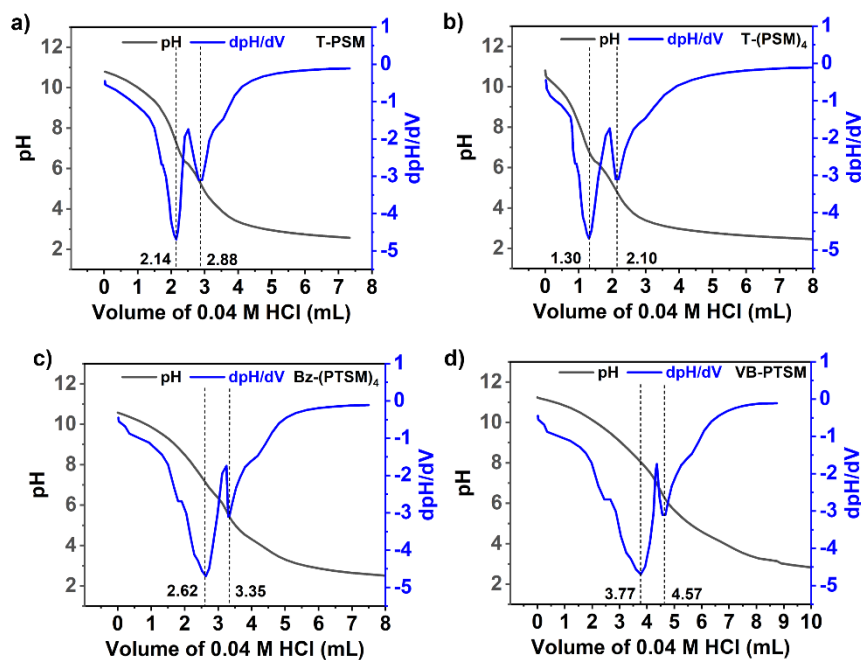
**Figure. S8** Potentiometric titration curves of (a) T-PSM, (b) T-(PSM)$_4$, (c) Bz-(PTSM)$_4$, and (d) VB-PTSM.

Determination of the amount of MAH unit in copolymer samples by potentiometric titration

With the continuous addition of 0.04 M HCl, two regions where pH declined suddenly appear on the potentiometric titration curves (Figure. S8). The two peaks in the dpH/dV curve show the two points with the fastest pH change during titration, which correspond to the two specific dissociation states of maleic acid groups. Therefore, the amount of HCl consumed between the two peaks corresponds to the amount of MAH unit contained in the copolymer samples.In Figure S8 (a), the $\Delta V_{HCl}$ = 0.74 mL , $n_{MAH} = \Delta V_{HCl} \times c_{HCl}$ = 29.6 μmol.

**Table S1** Results of potentiometric titration[a]

|  | T-PSM | T-(PSM)$_4$ | Bz-(PTSM)$_4$ | VB-PTSM |
|---|---|---|---|---|
| m[b]/mg | 6.90 | 7.34 | 6.98 | 6.91 |
| MAH[c] /μmol | 32.0 | 32.0 | 32.0 | 32.0 |
| HCl[d] /μmol | 29.6 | 32.0 | 29.2 | 32.0 |

[a] The hydrolyzed copolymer stock solution (2 mL) was diluted with deionized water to 40 mL, then brought to high pH by the addition of 0.5 M NaOH. The pH values with the addition of small volumes of 0.04 M HCl were recorded on a potentiometric titrator.

[b] Required mass of copolymer containing 32 μmol of MAH unit while assuming that the TPE-containing monomers and electron-rich monomers polymerized in alternating manner with MAH. Taking T-PSM as an example, the feeding ratio of T-PSM was [CTA]:[St]:[MAH]=1/40/40, and the molecular weight of T-PSM was $M_{n.th}$ = 8600 g/mol (Table 1). Therefore, the required mass of the T-PSM copolymer containing 32 $\mu$mol of MAH was calculated to be: $m = \frac{32 \text{ μmol}}{40} \times M_{n,th}$ = 6.9 mg.

[c] Calculated amount of MAH repeating unit while assuming that the TPE-containing monomers and St monomers polymerized in alternating manner with MAH.

[d] The molar amount of HCl consumed by one carboxylic acid group in maleic anhydride in a potentiometric titration. This amount was close to the calculated molar amount of maleic anhydride (32 μmol), indicating that TPE-containing monomers and electron-rich monomers are alternately polymerized with MAH.
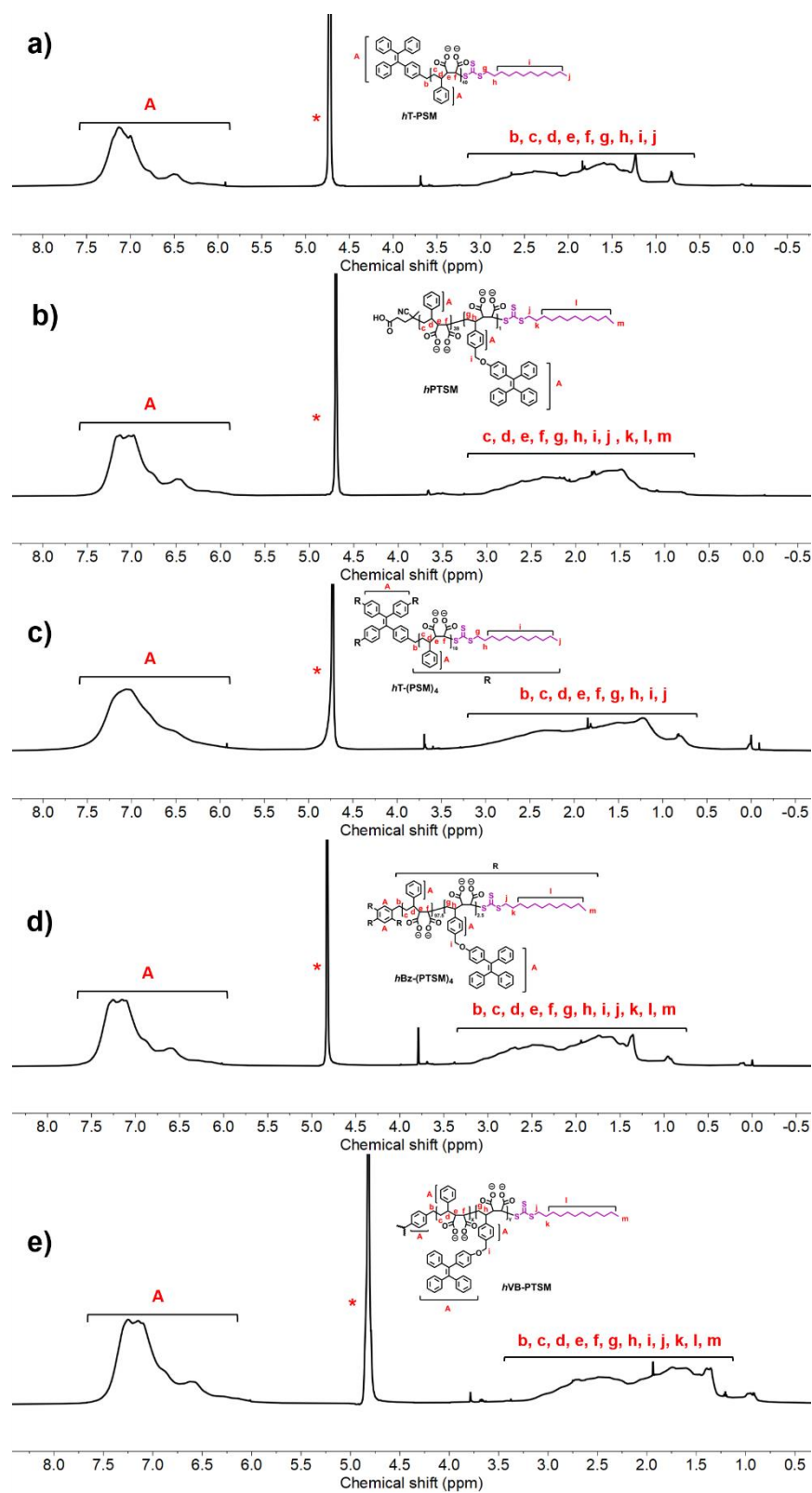
**Figure. S9** ^{1}H NMR spectra of (a) $h$T-PSM, (b) $h$PTSM, (c) $h$T-(PSM)$_4$, (d) $h$Bz-(PTSM)$_4$, and (e) $h$VB-PTSM in D$_2$O (pH = 12).
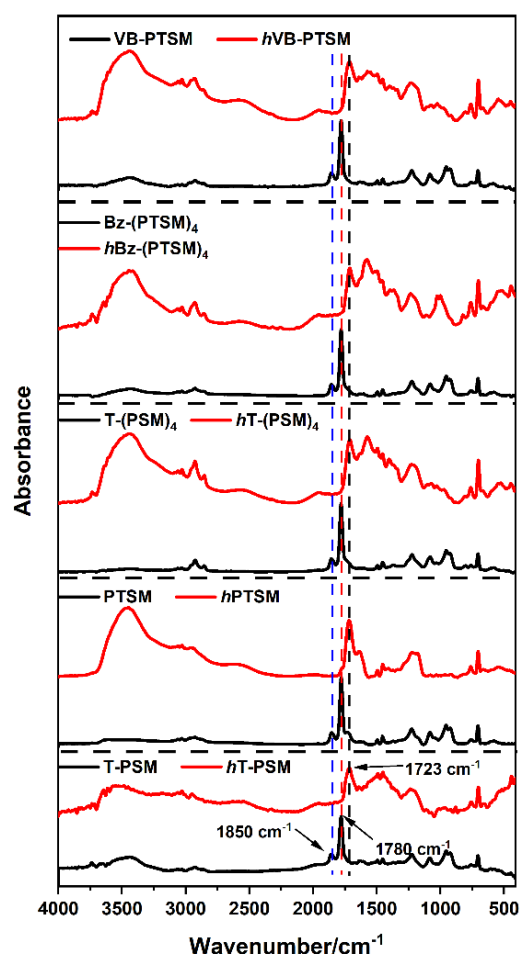
8

**Figure. S10** FTIR spectra of the TPE-appended maleic anhydride copolymers and their hydrolysates.
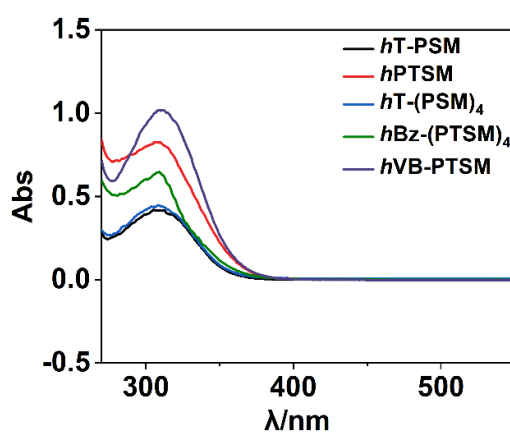


**Figure. S11** UV-vis absorption spectra of $h$T-PSM, $h$PTSM, $h$T-(PSM)$_4$, $h$Bz-(PTSM)$_4$, and $h$VB-PTSM in water.
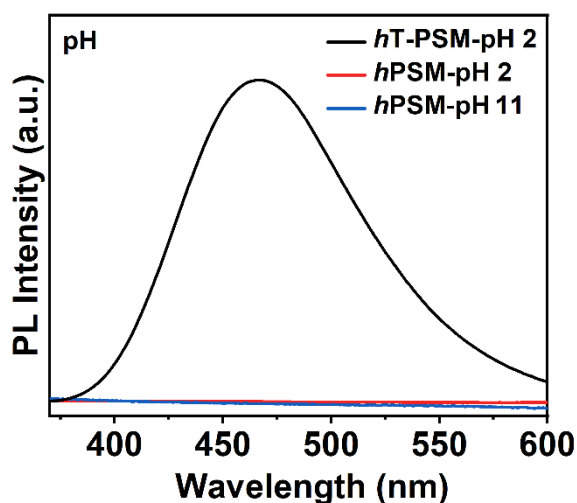
**Figure. S12** PL spectra of *h*T-PSM (pH =2) and *h*PSM (pH =2 and 11, blank groups) in
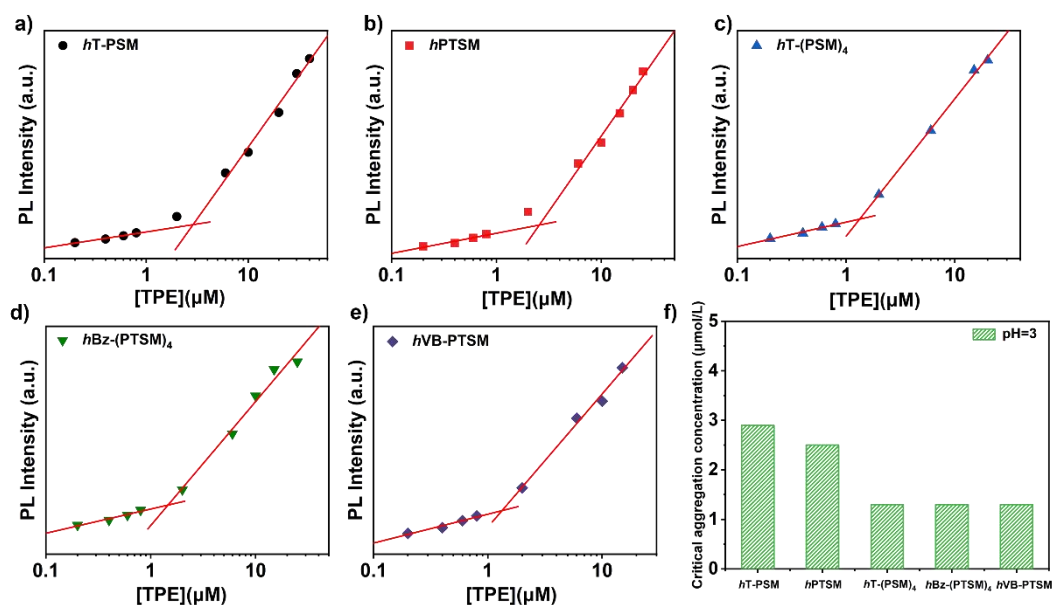
B−R buffer solutions.



**Figure. S13** PL intensity of (a) *h*T-PSM, (b) *h*PTSM, (c) *h*T-(PSM)$_4$, (d) *h*Bz-(PTSM)$_4$, and

(e) *h*VB-PTSM in the B−R buffer solutions (pH = 3) with different TPE concentration. (f)

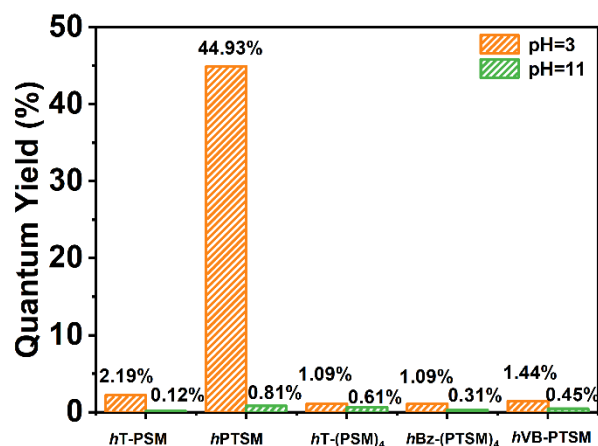Critical aggregation concentration of the five copolymers.

**Figure. S14** Absolute fluorescence QYs (Φ) of the five copolymers at pH = 3 and 11.

**Table S2.** Polymerization recipe, conversion, and GPC results of T-PSM with different targeted DP

| entry | [CTA]:[St]: [MAH]:[AIBN] | CTA | [M]/ wt% | Conv./ %[a] | $M_{n.th}$ (g/mol)[b] | $M_{n.GPC}$ (g/mol) | $Đ^e$ |
|---|---|---|---|---|---|---|---|
| T-PSM-40 | 1:40:40:0.05 | TPE-TTC | 30 | 99.4 | 8600 | 12200 | 1.26 |
| T-PSM-80 | 1:80:80:0.05 | TPE-TTC | 30 | 95.7 | 16100 | 18200 | 1.37 |
| T-PSM-160 | 1:160:160:0.05 | TPE-TTC | 30 | 86.8 | 28600 | 31700 | 1.38 |
| T-PSM-320 | 1:320:320:0.1 | TPE-TTC | 30 | 78.3 | 51000 | 54900 | 1.39 |

[a] Measured by $^1$H NMR.

[b] $M_{\mathrm{n,th}} = M_{\mathrm{w,CTA}} + C \times \dfrac{M_{\mathrm{w,St}} \times n_{\mathrm{St}} + M_{\mathrm{w,MAH}} \times n_{\mathrm{MAH}}}{n_{\mathrm{CTA}}}$

**Table S3.** Summary of the pH-responsive fluorescence performance of $h$T-PSM with different targeted DP

| entry | pH$_{50}{}^{a}$ | pH$_0{}^{b}$ | dynamic range |
|---|---|---|---|
| $h$T-PSM-40 | 4.19 | 5.43 | 59 |
| $h$T-PSM-80 | 4.39 | 5.48 | 108 |
| $h$T-PSM-160 | 4.20 | 5.55 | 142 |
| $h$T-PSM-320 | 4.36 | 5.54 | 133 |

[a] The pH value where half of the PL intensity enhancement was attained.

[b] The pH value of the intersect of the fitted lines of the steeper and flatter (weak emission) parts in Figure S15 e.
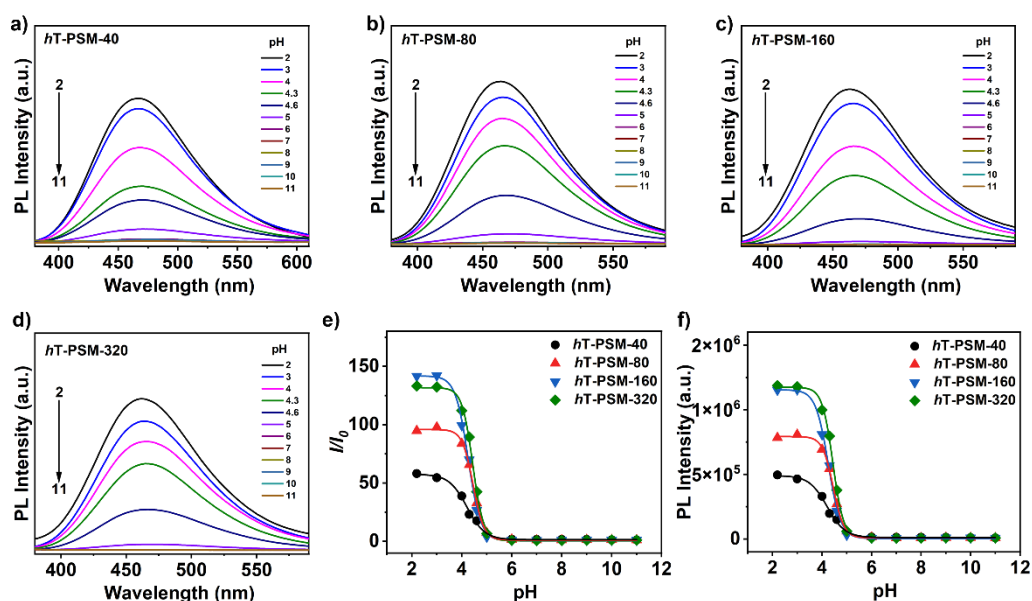


**Figure. S15** PL spectra of (a) $h$T-PSM-40, (b) $h$T-PSM-80, (c) $h$T-PSM-160, (d) $h$T-PSM-320 in the B−R buffer solutions of different pH. (e) Plots of $I/I_0$ vs pH. (f) Plots of PL intensity vs pH. [TPE] = 20 μM; excitation wavelength: 320 nm; $I_0$: the PL intensity of the corresponding copolymer in B−R buffer solutions at pH = 11.
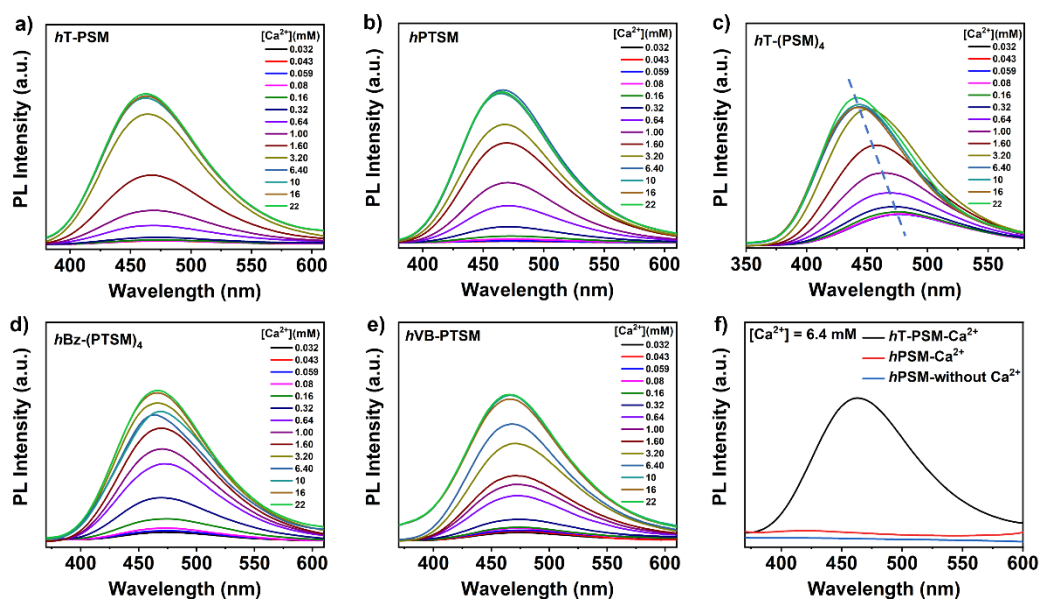
**Figure. S16** PL spectra of (a) $h$T-PSM, (b) $h$PTSM, (c) $h$T-(PSM)$_4$, (d) $h$Bz-(PSM)$_4$, and (e) $h$VB-PTSM in HEPES buffer solutions (70 mM, pH = 7.4) at different [Ca$^{2+}$]. [TPE] = 20 μM. (f) $h$T-PSM ([Ca$^{2+}$]=6.4 mM) and $h$PSM ([Ca$^{2+}$]=6.4 mM and without Ca$^{2+}$, blank groups) in HEPES buffer solutions (70 mM, pH = 7.4).

Determination of the apparent dissociation constant $K_d$.

By measuring the fluorescence intensity at different Ca$^{2+}$ concentrations, the $K_d$ can be obtained using the following Hill equation:

$$(I - I_{min})K_d + (I - I_{min})[Ca^{2+}]^n = (I_{max} - I_{min})[Ca^{2+}]^n \qquad \text{(Eq. S1)}$$

$I$: fluorescence intensity

$I_{max}$: maximum fluorescence intensity

$I_{min}$: minimum fluorescence intensity

$K_d$: apparent dissociation constant

n: apparent Hill coefficient

**Table S4.** Fluorescence dynamic range and apparent dissociation constants $K_d$ of $h$T-PSM with different targeted DP derived from the $Ca^{2+}$ titration experiments

| entry | apparent $K_d$ (mM) | $[Ca^{2+}]_{50}$ (mM) [a] | $n$ | dynamic range |
|---|---|---|---|---|
| $h$T-PSM-40 | 3.40 | 1.79 | 1.96 | 33 |
| $h$T-PSM-80 | 13.42 | 2.38 | 2.23 | 92 |
| $h$T-PSM-160 | 72.51 | 2.92 | 3.41 | 189 |
| $h$T-PSM-320 | 133.62 | 3.60 | 3.00 | 230 |

[a] The $[Ca^{2+}]$ where half of the PL intensity enhancement was attained.
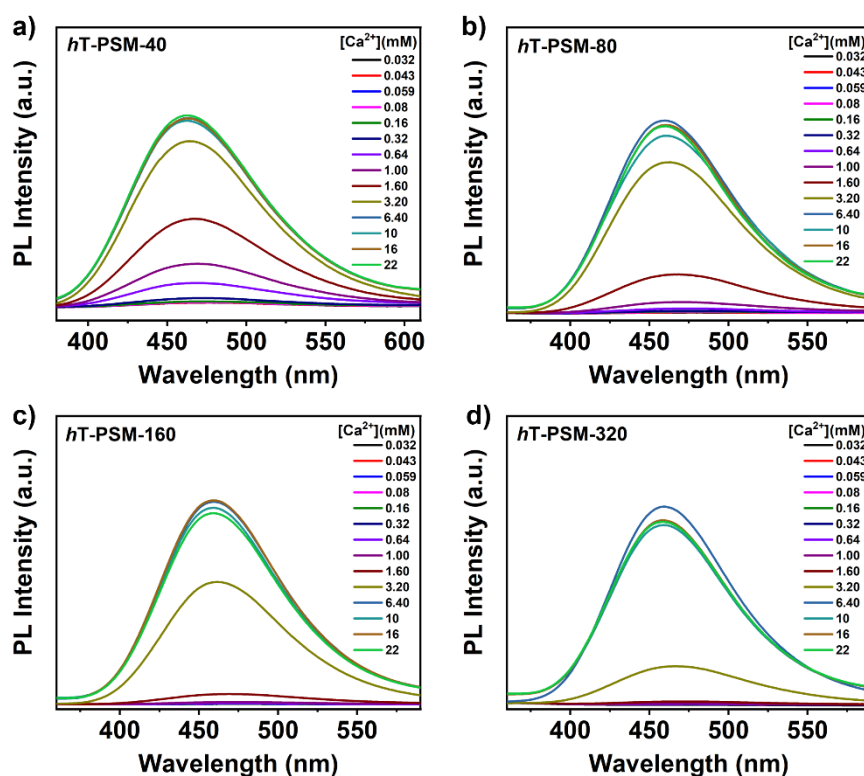


**Figure. S17** PL spectra of (a) $h$T-PSM-40, (b) $h$T-PSM-80, (c) $h$T-PSM-160, (d) $h$T-PSM-320 in HEPES buffer solutions (70 mM, pH = 7.4) at different $[Ca^{2+}]$. [TPE] = 20 μM.
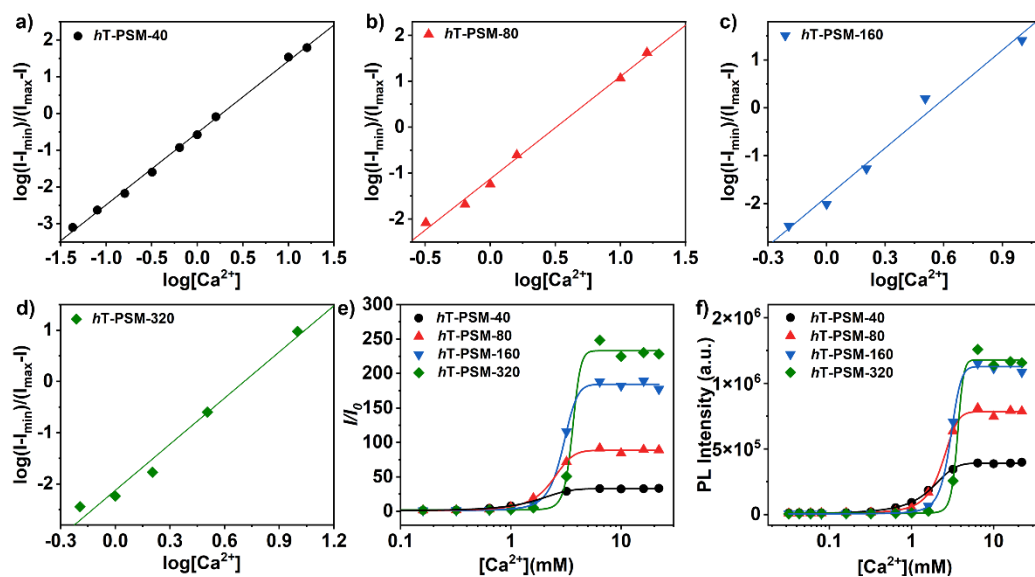
**Figure. S18** The corresponding Hill plots of (a) $h$T-PSM-40, (b) $h$T-PSM-80, (c) $h$T-PSM-160, (d) $h$T-PSM-320 in HEPES buffer solutions (70 mM, pH = 7.4) at different $[Ca^{2+}]$. (e) Plots of $I/I_0$ vs $Ca^{2+}$. (f) Plots of PL intensity vs $Ca^{2+}$. [TPE] = 20 μM; $I_0$: the PL intensity of the corresponding copolymer at $[Ca^{2+}]$ = 0.032 mM.
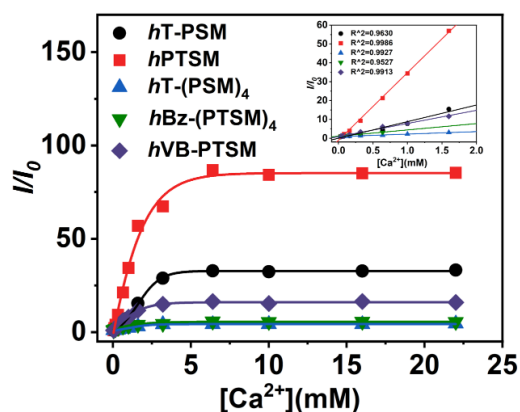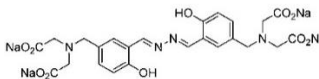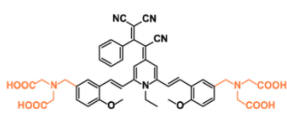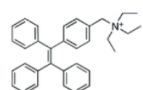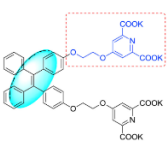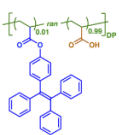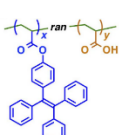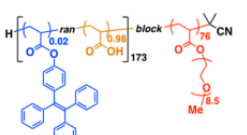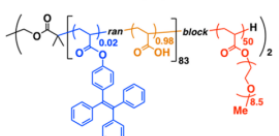


**Figure. S19** $I/I_0$ of $h$T-PSM, $h$PTSM, $h$T-(PSM)$_4$, $h$Bz-(PTSM)$_4$, and $h$VB-PSM in HEPES buffer solutions (70 mM, pH = 7.4) at different $[Ca^{2+}]$. [TPE] = 20 μM. Inset: linear region of the binding isotherm of $h$T-PSM, $h$PTSM, $h$T-(PSM)$_4$, $h$Bz-(PTSM)$_4$, and $h$VB-PSM to $Ca^{2+}$.

**Table S5.** Comparison of the performance of AIE-type fluorescent $Ca^{2+}$ probes in the

literature and the TPE-containing maleic acid copolymers in our work

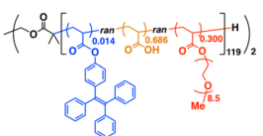| Fluorescent probe structure | [AIE] ($\mu$M) [a] | [$Ca^{2+}$] (mM) [b] | dynamic range [c] | Linear range (mM) [d] | ref |
|---|---|---|---|---|---|
|  | 1 | 3 | 12 | 0-3.0 | 2 |
|  | 1000 | 4.8 | 21 | 0.2–4.8 | 3 |
|  | 1 | 1 | 5 | 0-0.1 | 4 |
|  | 20 | 0.01 | 9 | 0-0.012 | 5 |
|  | 19 | 5 | 68 | 0-2.0 | 6 |
|  | 12 | 9 | 69 | 0-4.5 | 7 |
|  | 0.7 | 20 | 1.4 | 0-10 | 8 |
|  | 1.0 | 20 | 21 | 0-10 | 8 |
|  | 0.9 | 20 | 7.1 | 0-10 | 8 |

| | $a$ | $b$ | $c$ | $d$ | |
|---|---|---|---|---|---|
|  | 1.9 | 50 | 24 | 0-10 | 8 |
|  | 20 | 6.4 | 15 | 0-3.2 | 9 |
|  | 20 | 1.0 | 17 | 0-0.64 | 9 |
| $h$T-PSM | 20 | 6.4 | 33 | 0-3.2 | |
| $h$PTSM | 20 | 6.4 | 86 | 0-1.6 | This work |
| $h$T-(PSM)$_4$ | 20 | 6.4 | 4 | 0-1.6 | |
| $h$Bz-(PTSM)$_4$ | 20 | 6.4 | 14 | 0-0.64 | |
| $h$VB-PTSM | 20 | 6.4 | 14 | 0-1.6 | |

$a$ Concentration of AIEgen in fluorescence tests.

$b$ Maximum $Ca^{2+}$ concentration with monotonic fluorescence response.

$c$ Dynamic range at maximum $Ca^{2+}$ concentration.

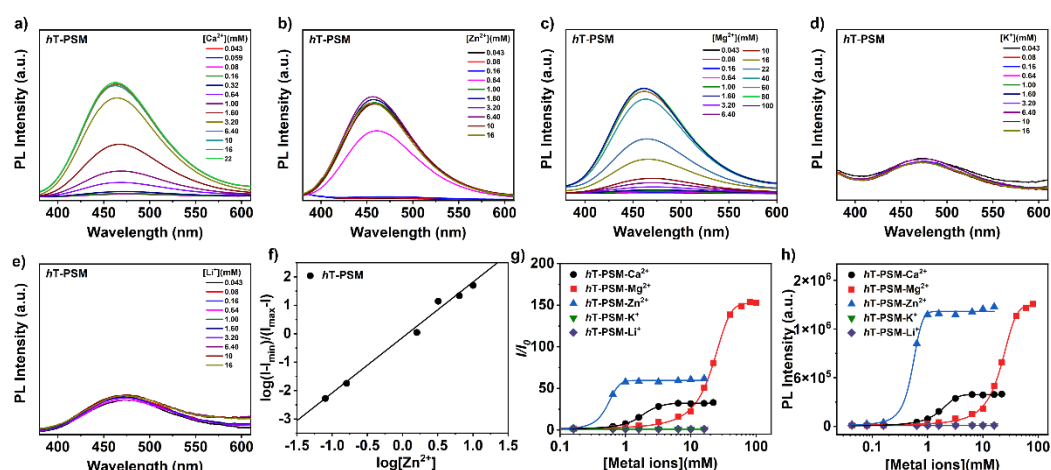$d$ $Ca^{2+}$ concentration range with linearly enhanced fluorescence intensity.

**Figure. S20** PL spectra of $h$T-PSM in HEPES buffer solutions (70 mM, pH = 7.4) at different (a) [Ca$^{2+}$], (b) [Zn$^{2+}$], (c) [Mg$^{2+}$], (d) [K$^+$], (e) [Li$^+$]. (f) Hill plot of $h$T-PSM in Tris buffer solutions (70 mM, pH = 7.4) at different [Zn$^{2+}$]. (g) Plots of $I/I_0$ vs [metal ions]. (h) Plots of PL intensity vs [metal ions]. [TPE] = 20 μM; $I_0$: the PL intensity of the corresponding copolymer at [metal ions] = 0.043 mM. Tris buffer solutions (70mM, pH = 7.4) was used in the case of Zn$^{2+}$ because of its precipitation in HEPES buffer solution.

**Table S6.** Fluorescence dynamic range and apparent dissociation constants $K_d$ of the $h$T-PSM maleic acid copolymer derived from the metal ions titration experiments

| $h$T-PSM | Apparent $K_d$ (mM) | [Metal ions]$_{50}$ (mM)$^a$ | $n$ | Dynamic range |
|---|---|---|---|---|
| Ca$^{2+}$ | 3.40 | 1.75 | 1.96 | 33 |
| Mg$^{2+}$ | 58.61 | 21.45 | 1.16 | 154 |
| Zn$^{2+}$ | 1.35 | 0.54 | 1.95 | 62 |
| K$^+$ | / | / | / | 1.1 |
| Li$^+$ | / | / | / | 1.1 |

$^a$The [Metal ions] where half of the PL intensity enhancement was attained.

18
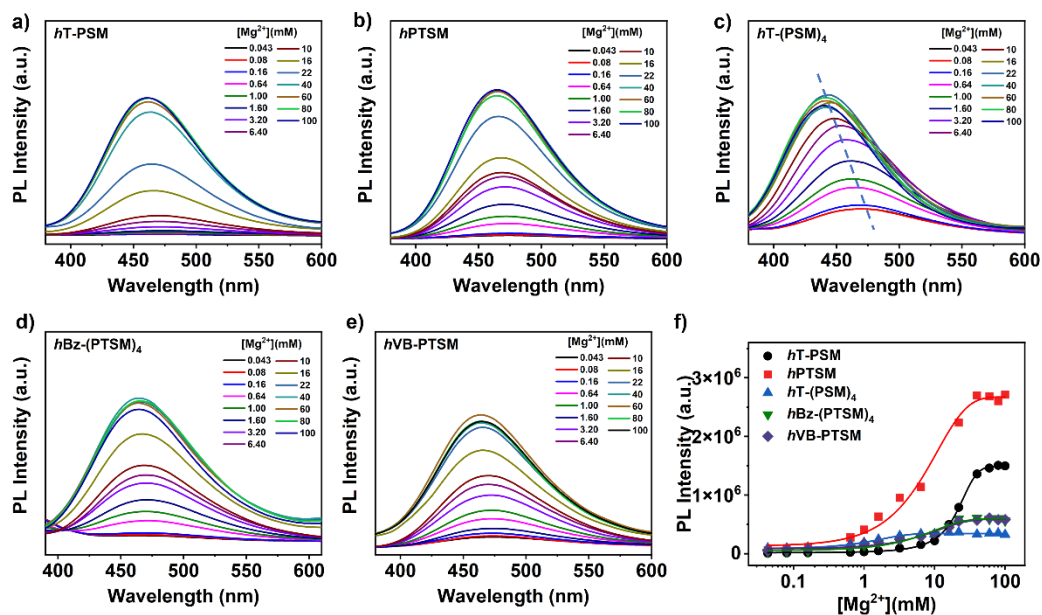
**Figure. S21** PL spectra of (a) *h*T-PSM, (b) *h*PTSM, (c) *h*T-(PSM)$_4$, (d) *h*Bz-(PTSM)$_4$, and (e) *h*VB-PTSM in HEPES buffer solutions (70 mM, pH = 7.4) at different [Mg$^{2+}$]. (f) Plots of PL intensity vs Mg$^{2+}$. [TPE] = 20 μM.

**Figure 22.** Hill plots of (a) $h$T-PSM, (b) $h$PTSM, (c) $h$T-(PSM)$_4$, (d) $h$Bz-(PTSM)$_4$, and (e) $h$VB-PTSM in HEPES buffer solutions (70 mM, pH = 7.4) at different [M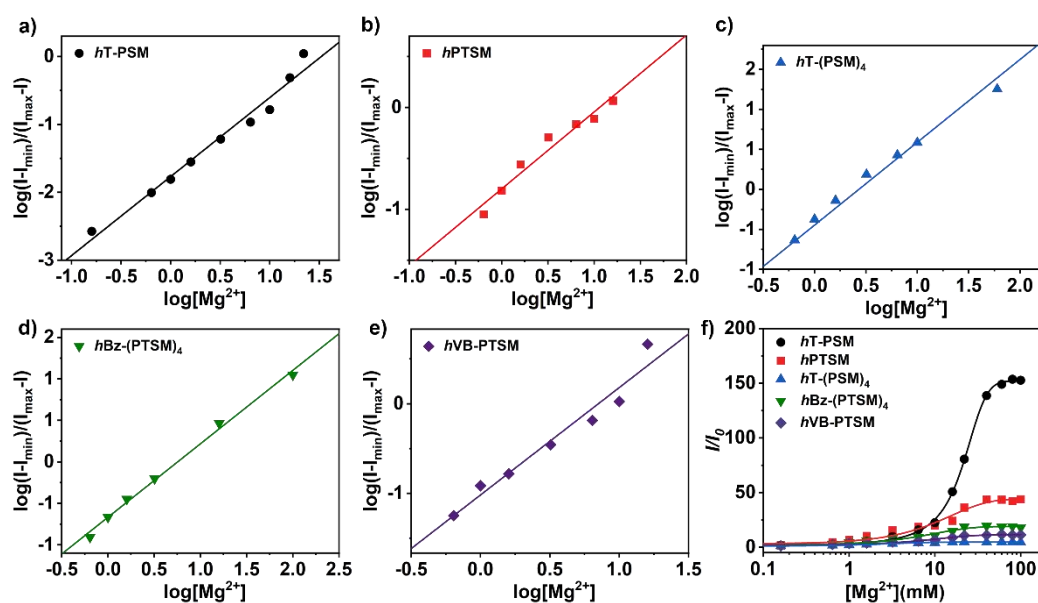g$^{2+}$]. (f) Plots of $I/I_0$ vs Mg$^{2+}$. [TPE] = 20 μM. $I_0$: the PL intensity of the corresponding copolymer at [Mg$^{2+}$] = 0.043mM.

**Table S7.** Fluorescence dynamic range and apparent dissociation constants $K_d$ of the five maleic acid copolymers derived from the Mg$^{2+}$ titration experiments

| Entry | Apparent $K_d$ (mM) | [Mg$^{2+}$]$_{50}$ (mM)$^a$ | $n$ | Dynamic range |
|---|---|---|---|---|
| $h$T-PSM | 58.61 | 21.45 | 1.16 | 154 |
| $h$PTSM | 6.30 | 10.04 | 0.76 | 44 |
| $h$T-(PSM)$_4$ | 2.80 | 1.17 | 1.04 | 5 |
| $h$Bz-(PTSM)$_4$ | 4.66 | 6.02 | 0.89 | 19 |
| $h$VB-PTSM | 4.08 | 6.68 | 0.72 | 12 |

$^a$The [Mg$^{2+}$] where half of the PL intensity enhancement was attained.
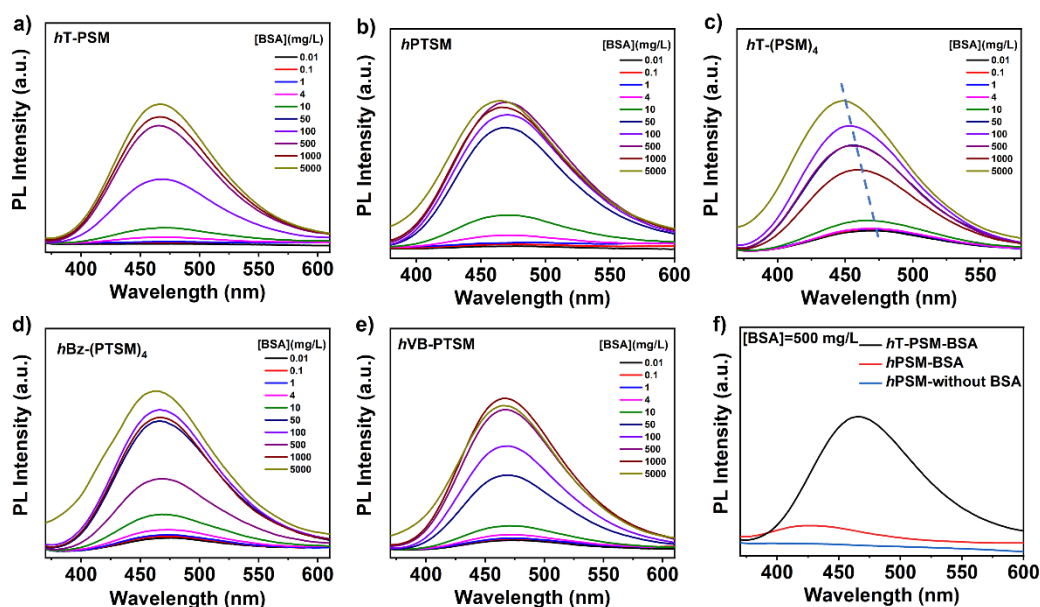
20

**Figure. S23** PL spectra of (a) $h$T-PSM, (b) $h$PTSM, (c) $h$T-$(PSM)_4$, (d) $h$Bz-$(PTSM)_4$, and (e) $h$VB-PTSM in HEPES buffer solutions (70 mM, pH = 7.4) at different [BSA]. [TPE] = 2 μM. (f) $h$T-PSM ([BSA]=500 mg/L) and $h$PSM ([BSA]=500 mg/L and without BSA, blank groups) in HEPES buffer solutions (70 mM, pH = 7.4).

**Table S8.** Fluorescence dynamic range and apparent dissociation constants $K_d$ of $h$T-PSM with different targeted DP derived from the BSA titration experiments

| entry | apparent $K_d$ (mg/L) | $[BSA]_{50}$ (mg/L) [a] | $n$ | dynamic range |
|---|---|---|---|---|
| $h$T-PSM-40 | 85.66 | 38.36 | 1.20 | 114 |
| $h$T-PSM-80 | 90.43 | 56.55 | 1.07 | 187 |
| $h$T-PSM-160 | 235.93 | 67.81 | 1.18 | 81 |
| $h$T-PSM-320 | 407.69 | 80.46 | 1.29 | 95 |

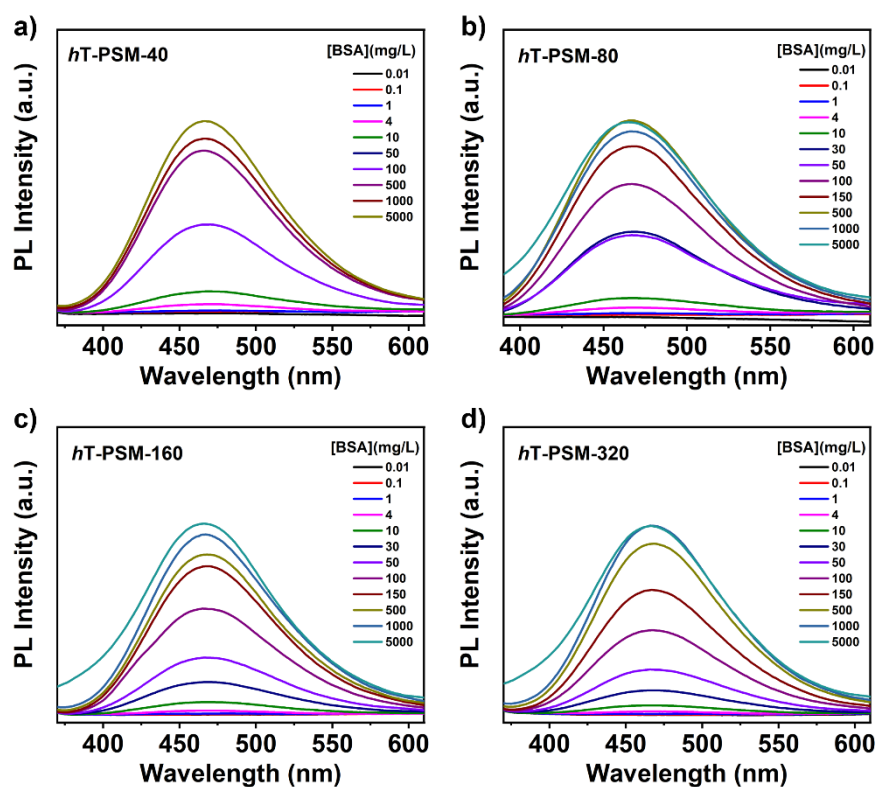[a] The [BSA] where half of the PL intensity enhancement was attained.

**Figure. S24** PL spectra of (a) *h*T-PSM-40, (b) *h*T-PSM-80, (c) *h*T-PSM-160, and (d) *h*T-PSM-320 in HEPES buffer solutions (70 mM, pH = 7.4) at different [BSA]. [TPE] = 2 μM.
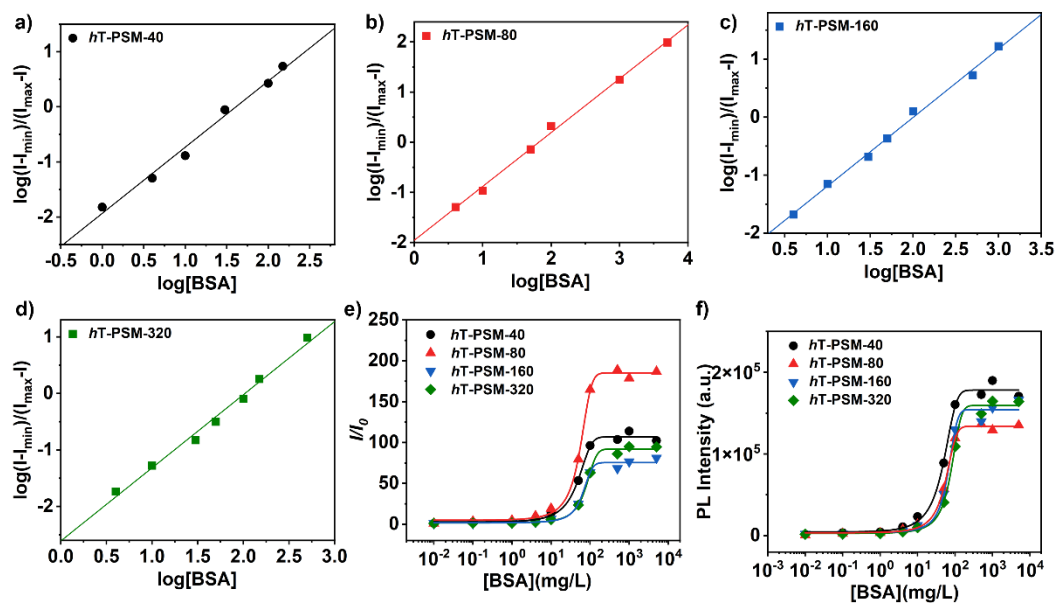
**Figure. S25** The corresponding Hill plots of (a) $h$T-PSM-40, (b) $h$T-PSM-80, (c) $h$T-PSM-160, (d) $h$T-PSM-320 in HEPES buffer solutions (70 mM, pH = 7.4) at different [BSA]. (e) Plots of $I/I_0$ vs BSA. (f) Plots of PL intensity vs BSA. [TPE] = 2 μM; $I_0$: the PL intensity of the corresponding copolymer at [BSA] = 0.01 mg/L.

### References

1. N. T. H. Ha, *Polymer*, 1999, **40**, 1081-1086.

2. M. Gao, Y. Li, X. Chen, S. Li, L. Ren and B. Z. Tang, *ACS Appl. Mater. Interfaces*, 2018, **10**, 14410-14417.

3. X. Li, C. Pan, J. Cao, Z. Liu, Z. Zhu, C. Yan, W. Zhao, W.-H. Zhu and Q. Wang, *Biomaterials*, 2022, **289**, 121778.

4. R. Wang, X. Du, X. Ma, J. Zhai and X. Xie, *Analyst*, 2020, **145**, 3846-3850.

5. J. Zhang, Z. Yan, S. Wang, M. She, Z. Zhang, W. Cai, P. Liu and J. Li, *Dyes. Pigm.*, 2018, **150**, 112-120.

6. K. Morishima, F. Ishiwari, S. Matsumura, T. Fukushima and M. Shibayama, *Macromolecules*, 2017, **50**, 5940-5945.

7. F. Ishiwari, H. Hasebe, S. Matsumura, F. Hajjaj, N. Horii-Hayashi, M. Nishi, T. Someya and T. Fukushima, *Sci. Rep-UK*, 2016, **6**, 24275.

8. F. Ishiwari, M. Sakamoto, S. Matsumura and T. Fukushima, *ACS Macro Lett.*, 2018, **7**, 711-715.

9. X. Guo, T. Song, D. Chen, J. Zhu, Z. Li, Q. Xia, L. Wang and W. Yang, *ACS Appl. Mater. Interfaces*, 2023, **15**, 3543-3557.